

# Appendix B

## Numerical uniform approximation

The uniform approximation as presented by Schomerus and Sieber [70, 73] requires knowledge about the properties of the ghost orbits. This information is not available in a numerical calculation. Therefore it is desirable to develop a modified approach which only needs data that can be accessed numerically.

The derivation of Sieber and Schomerus starts from the normal form of the bifurcation. They express their parameters in terms of the quantities which enter the Gutzwiller trace formula. On the side of the bifurcations where all orbits are real, their formulas can directly be evaluated numerically. In the following, a technique for a numerical access to the complex side is presented. It consists of a fit of the parameters of the local form. The normal form is then extrapolated to the complex regime in a way that ensures the correct limiting behavior far from the bifurcation. This makes the numerical approach uniform in the sense that both the local behavior at the bifurcation and the Gutzwiller limit are reproduced correctly.

This procedure is derived for the two types of bifurcations occurring in the channel system, namely the tangent (or isochronous) and the period doubling (or pitchfork) bifurcation.

### B.1 Tangent bifurcation

The normal form of the tangent bifurcation implies the following local behavior of the action<sup>1</sup>  $S$  and the amplitudes  $A$  of the two orbits engaged in the bifurcation [70]:

$$\begin{aligned} S_{1,2} &= S_0 \mp \frac{2\varepsilon}{3} \sqrt{-\frac{\varepsilon}{3a} - \frac{b\varepsilon^2}{9a^2}}, \\ A_{1,2} &= \frac{1}{|12a\varepsilon|^{1/4}} \left( A_0 \mp \gamma \sqrt{-\frac{\varepsilon}{3a}} \right). \end{aligned} \tag{B.1}$$

Considering the level density,  $A_0$  is given by the period  $T_0$  of the orbit; in case of the conductance,  $A_0$  is the velocity-velocity correlation function (see Eqs. (2.14) and (5.4)).  $\varepsilon$  is the parameter which is varied across the bifurcation. It is zero at the bifurcation

---

<sup>1</sup>For a simple notation, the actions are given in units of  $\hbar$  in this appendix.

itself and negative on the real side (i. e. the side of the bifurcation where the orbits exist classically). It will be convenient to define the quantities

$$\begin{aligned}\bar{A} &:= \frac{A_1 + A_2}{2A_0}; & \Delta A &:= \frac{A_1 - A_2}{2A_0}; \\ \bar{S} &:= \frac{S_1 + S_2}{2}; & \Delta S &:= \frac{S_1 - S_2}{2}.\end{aligned}\tag{B.2}$$

Using that  $S_0$  generically has a dominant linear dependence on  $\varepsilon$ , the local behavior at the bifurcation according to Eq. (B.1) can be written as

$$\begin{aligned}|\bar{A}|^{-4} &= \alpha_1 |\varepsilon|; & |\Delta A|^4 &= \alpha_2 |\varepsilon|; \\ \bar{S} &= \bar{S}_0 + \alpha_4 \varepsilon; & |\Delta S|^{2/3} &= \alpha_3 |\varepsilon|.\end{aligned}\tag{B.3}$$

For  $\Delta A$  the higher-order terms in  $\varepsilon$  stemming from a variation of  $\gamma$  are neglected here. Either of the first three relations can be used to define the mapping between  $\varepsilon$  and the physical quantity varied across the bifurcation (which is the magnetic field  $B$  in the present system). This mapping has to be extrapolated to the complex region. For the system considered in this work, the linear term of this mapping strongly dominates, so that higher-order contributions could be neglected. This approximation is equivalent to the ansatz

$$\varepsilon = \beta(B - B_{\text{bif}}).\tag{B.4}$$

The linear relations Eqs. (B.3) together with Eq. (B.4) allow to determine the parameters  $\alpha_{1-4}$ ,  $\bar{S}_0$  and  $B_{\text{bif}}$  using straight-line fits.<sup>2</sup> This is numerically more convenient than using the original expressions Eqs. (B.1). Data points close to the bifurcations have a limited numerical accuracy, since it is difficult to converge to a marginally stable orbit (there the technique using the stability matrix fails due to vanishing first derivatives). Far from the bifurcation, the leading-order approximations of Eq. (B.1) no longer hold. So prior to the fit of the parameters of the local normal form, the fit region has to be adapted. Straight-line fits are numerically very stable and can be used both for the determination of the optimal fit region and for the fit of the parameter themselves. The upper as well as the lower limit of the fit-range were chosen for a minimal error in the slopes.

Eqs. (B.3) give only the absolute values for  $\bar{A}$ ,  $\Delta A$  and  $\Delta S$ . The signs of these quantities can be omitted if the following factors are introduced:

$$\sigma_1 := \text{sign}(\Delta S); \quad \sigma_2 := \text{sign}(\Delta A).\tag{B.5}$$

These are readily calculated on the real side of the bifurcation.

The Maslov index of the bifurcation is given by the average of the Maslov indices of the two orbits involved

$$\mu = (\mu_1 + \mu_1)/2.\tag{B.6}$$

---

<sup>2</sup>The parameters are actually over-determined by Eqs. (B.3), since  $B_{\text{bif}}$  can be extracted from either of the three first equations. This gives a convenient additional error control.

In these quantities the uniform approximation for the tangent bifurcation reads [70]

$$\delta = \sqrt{\frac{2\pi}{3}|\Delta S|} \times \left[ \begin{aligned} & |\bar{A}| \{J_{-1/3}(|\Delta S|) + J_{1/3}(|\Delta S|)\} \cos\left(\bar{S} - \mu\frac{\pi}{2}\right) \\ & - \sigma_1\sigma_2|\Delta A| \{J_{-2/3}(|\Delta S|) - J_{2/3}(|\Delta S|)\} \cos\left(\bar{S} - (\mu - 1)\frac{\pi}{2}\right) \end{aligned} \right] \quad (\text{B.7})$$

on the real side, and

$$\delta = \sqrt{\frac{2}{\pi}|\Delta S|} \times \left[ \begin{aligned} & |\bar{A}|K_{1/3}(|\Delta S|) \cos\left(\bar{S} - \mu\frac{\pi}{2}\right) \\ & - \sigma|\Delta A|K_{2/3}(|\Delta S|) \cos\left(\bar{S} - (\mu - 1)\frac{\pi}{2}\right) \end{aligned} \right] \quad (\text{B.8})$$

on the complex side. All prefactors (including the degeneracy) have been absorbed in the amplitudes  $A_i$ , so that the formulas are valid both for the level density and the conductance and also for systems with continuous symmetries.

On the real side far from the bifurcation, the uniform approximation Eq. (B.7) can, as already pointed out, be implemented directly in a numerical calculation. In this region,  $\bar{A}$ ,  $\Delta A$ ,  $\bar{S}$  and  $\Delta S$  can be determined from the properties of the classical orbits, using the definitions Eqs. (B.2). Close to the bifurcation the numerical evaluation of  $\Delta A$  fails, since the amplitudes diverge at this point. There, however, Eqs. (B.3) (with the parameters adapted as described above) yield the correct local behavior. This local form also holds for the complex side of the bifurcation. Since  $\Delta S$  increases like  $\varepsilon^{3/2}$ , the contribution on the complex side according to Eq. (B.8) goes to zero. This ensures that the numerical extrapolation reproduces the correct Gutzwiller limit on the complex side. The only difference to the analytic uniform approximation is the intermediate complex regime. There, however, the contributions are strongly suppressed, so that the deviation is small.

The crossover between the local normal form and the direct orbit data is preferably implemented by a linear interpolation between these two descriptions. Choosing for this crossover approximately half the region used for the parameter fit above, the crossover is smooth. This is simply because the two methods are by construction well adapted in this regime.

The results are depicted for a typical tangent bifurcation of the channel system in Fig. B.1. The action is scaled by a factor of 10 for clarity. The solid lines in the insets show the local behavior of the quantities of Eqs. (B.3). The corresponding linear fit<sup>3</sup> is indicated by the dashed line. The main graph shows the Gutzwiller result (thin) and the numerical uniform approximation (heavy), which reproduces the Gutzwiller data far from the bifurcation. The spurious divergence is, indeed, removed, and decaying contributions from ghost orbits are included.

---

<sup>3</sup>The plotted range in  $B$  is approximately 5 times the optimal fit region, so that the nonlinearities can clearly be seen.

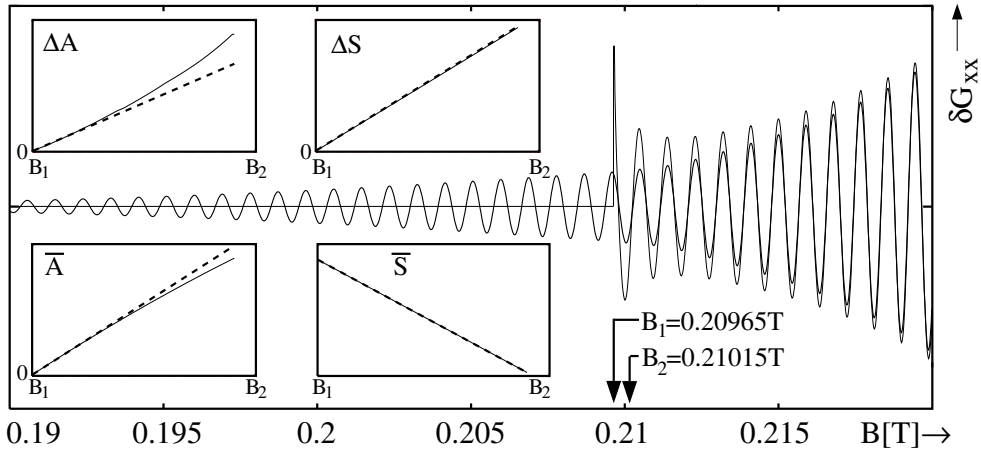


Figure B.1: The tangent bifurcation of Fig. 4.4, with action scaled by a factor of 10. Thin: Gutzwiller result, heavy: numerical uniform result. The insets show the behavior of the quantities of Eqs. (B.3) (solid) and their linear fit (dashed).

## B.2 Pitchfork bifurcation

The normal form of the period-doubling bifurcation implies the following local behavior:

$$\begin{aligned}
 S_1 &= S_0 + \frac{\varepsilon^2}{4a} \left(1 + \frac{c\varepsilon}{2}\right) \\
 \text{Tr}_0 &:= \text{Tr}(M_0) = 2 - 2\sigma\varepsilon \\
 \text{Tr}_1 &:= \text{Tr}(M_1) = 2 + 4\sigma\varepsilon - 3c\sigma\varepsilon^2.
 \end{aligned} \tag{B.9}$$

Here (and in the following) the subscript 0 denotes the central orbit, and the subscript 1 the two orbits<sup>4</sup> that split off at the bifurcation. In contrast to the tangent bifurcation discussed above, here the central orbit is real on both sides of the bifurcation. Therefore the mapping between  $\varepsilon$  (the parameter of the normal form driving the system through the bifurcation) and  $B$  (the physical parameter varied across the bifurcation) can be left implicit by substituting  $\varepsilon$  with  $\sigma(1 - \text{Tr}_0/2)$ .

It is again necessary to carefully adapt the fit ranges, since both close to and far from the bifurcation the errors increase. Therefore the parameters are again determined using suitable linear relations. The absolute value of the parameter  $c$  is readily fitted by

$$\sqrt{6 - (2\text{Tr}_0 + \text{Tr}_1)} = \sqrt{|3c|} |1 - \text{Tr}_0/2|. \tag{B.10}$$

It is convenient to define the factors  $\sigma$ ,  $\sigma_1$  and  $\sigma_2$ , which only contain sign informations.  $\sigma_2$  is 1 on the real side (i. e. where both the central orbit and the satellites exist classically), and  $-1$  on the complex side of the bifurcation.  $\sigma$  and  $\sigma_1$  refer to properties of the real side of the bifurcation.  $\sigma_1$  is given by the sign of  $(S_1 - S_0)$ , and  $\sigma = \sigma_1$  if the central orbit is unstable, and  $\sigma = -\sigma_1$  otherwise. The sign of  $c$  can be determined on the real side by

$$\text{sign}(c) = \sigma \text{sign}[6 - (2\text{Tr}_0 + \text{Tr}_1)]. \tag{B.11}$$

<sup>4</sup>This corresponds to the channel with antidots considered in this work. For generic systems without discrete symmetries, there is one satellite orbit with twice the period.

Using

$$\Delta S := \frac{S_1 - S_0}{2} = \frac{1}{8a} \left(1 - \frac{\text{Tr}_0}{2}\right)^2 \left[1 + \frac{c\sigma}{2} \left(1 - \frac{\text{Tr}_0}{2}\right)\right], \quad (\text{B.12})$$

the parameter  $a$  can be evaluated by another linear fit. The Maslov index  $\mu$  in the uniform approximation is given by the Maslov index of the central orbit where it is unstable.<sup>5</sup> The uniform approximation for the period doubling bifurcation is most easily written down defining the amplitudes

$$A_i = \frac{k_i}{\sqrt{|\text{Tr}_i - 2|}}, \quad (\text{B.13})$$

(where the  $k_i$  contain all prefactors of the trace formula, including the degeneracy of the orbit) and their linear combinations

$$A^+ := \left(\frac{A_1}{2} + \frac{A_0}{\sqrt{2}}\right) \quad \text{and} \quad A^- := \left(\frac{A_1}{2} - \frac{A_0}{\sqrt{2}}\right). \quad (\text{B.14})$$

Using these quantities, the uniform approximation reads [70]

$$\begin{aligned} \delta = \sqrt{\frac{\pi}{2}|\Delta S|} \mathcal{R}e \left[ \exp\left(i\left\{\bar{S} - \mu\frac{\pi}{2} - \sigma\frac{\pi}{4}\right\}\right) \times \right. \\ \left. \left\{ A^+ \left( \sigma_2 J_{1/4}(|\Delta S|) e^{i\sigma_1 \pi/8} + J_{-1/4}(|\Delta S|) e^{-i\sigma_1 \pi/8} \right) \right. \right. \\ \left. \left. + A^- \left( J_{3/4}(|\Delta S|) e^{i\sigma_1 3\pi/8} + \sigma_2 J_{-3/4}(|\Delta S|) e^{-i\sigma_1 3\pi/8} \right) \right\} \right]. \end{aligned} \quad (\text{B.15})$$

The numerical evaluation is similar to the case of the tangent bifurcation. On the side where all orbits are real,  $A^+$ ,  $A^-$ ,  $\Delta S$  and  $\bar{S}$  can be determined directly from the numerical orbit data. Near the bifurcation, where the amplitudes diverge and their near-cancellation causes numerical problems,  $A^\pm$  can be approximated via

$$\begin{aligned} A^+ &= \frac{k_0}{2\sqrt{|1 - \text{Tr}_0/2|}} \left( \frac{2}{\sqrt{|4 - 3c\sigma(1 - \text{Tr}_0/2)|}} + 1 \right) \\ A^- &= \frac{k_0}{2\sqrt{|1 - \text{Tr}_0/2|}} \left( \frac{2}{\sqrt{|4 - 3c\sigma(1 - \text{Tr}_0/2)|}} - 1 \right). \end{aligned} \quad (\text{B.16})$$

Here it was used that  $k_1 = 2k_0$  at the bifurcation.  $\Delta S$  can directly be extrapolated with Eq. (B.12), and  $\bar{S}$  via  $\bar{S} := (S_0 + S_1)/2 = S_0 + \Delta S$ . These formulae can also be used on the complex side in the vicinity of the bifurcation. To ensure the correct Gutzwiller limit on that side, the numerically determined properties of the central orbit should be used far from the bifurcation.  $\bar{S}$  and  $\Delta S$  can be calculated as above, and the ghost amplitude is extrapolated by

$$A_1 = \frac{2k_0}{\sqrt{|1 - \text{Tr}_0/2|}} \frac{1}{\sqrt{|4 - 3c\sigma(1 - \text{Tr}_0/2)|}}. \quad (\text{B.17})$$

---

<sup>5</sup>The central orbit is unstable on the real side of the bifurcation if  $\sigma\sigma_1 = 1$  and on the complex side otherwise.

These approximations are only valid for  $c\sigma(1 - \text{Tr}_0/2) \ll 4/3$ . At  $c\sigma(1 - \text{Tr}_0/2) = 4/3$  the local expansions of  $\Delta S$  and  $A_1$  exhibit a spurious divergence. If on the complex side  $c\sigma(1 - \text{Tr}_0/2) > 0$ , this leads to a spurious divergence of the numerical bifurcation treatment. The limit far from the bifurcations, however, is reproduced correctly<sup>6</sup>. In this work, the spurious divergence therefore was simply suppressed. Again, the error introduced is tolerable, since both the local behavior at the bifurcation and the Gutzwiller limit for isolated orbits is correctly reproduced. In the intermediate complex regime, where the inclusion of the ghost orbit in the numerical approach is not exact, its contribution is suppressed with  $a|1 - \text{Tr}_0/2|^{-5/2}$ .

The result of the numerical treatment of a period doubling bifurcation for the channel system is plotted in Fig. 4.4(b,c) of Sec. 7.4.4.2. As for the tangent bifurcation, far from the bifurcation the Gutzwiller contributions are reproduced, and the divergence at the bifurcation is removed.

---

<sup>6</sup>For  $\Delta S \rightarrow \infty$  the satellite terms in Eq. (B.15) exactly cancel.